π-N Scattering with Inelastic Contributions

L. F. Cook, Jr.*
Palmer Physical Laboratory, Princeton University, Princeton, New Jersey

AND

B. W. Lee†‡
Institute for Advanced Study, Princeton, New Jersey

(Received January 18, 1962)

The N/D formulation of the unitarity S matrix, valid for reactions involving production processes, is applied to the reactions, $\pi+N\to\pi+N$, $\pi+N\to\pi+\pi+N$, $\pi+\pi+N\to\pi+\pi+N$, in the energy region of the higher resonances. A model is constructed in which the two pions in three-particle states interact in only one state, and the left-hand discontinuities of the elastic and three-particle scattering amplitudes are neglected while the left-hand discontinuities of the production amplitude are approximated by a pole. The elastic amplitude is driven through unitarity by the inelastic amplitude. The general properties of this model are investigated, and the procedure is applied to the D- and F-wave scattering of the $\pi-N$ system. The comparison between the experimental data and the model presented here is quite favorable.

I. INTRODUCTION

In this paper we shall apply the formalism developed in the previous paper[1] to pion-nucleon scattering and pion-production in the sub-BeV region. More specifically, we would like to explore the possibility that the higher resonances in elastic scattering are driven, through unitarity, by a growing production process. Indeed such a mechanism is well known in nuclear reaction theory.[2] A related point of view was taken by Ball and Frazer,[3] who show that the second and third resonances in pion-nucleon scattering are what Nauenberg and Pais[4] call "wooly" cusp effects; the effects are associated with the opening of the production channel consisting of a nucleon and an unstable vector meson which subsequently decays strongly into two pions.

What we would like to demonstrate is that the contribution from the inelastic channels can cause a resonance in the elastic channel, *even below the threshold of the inelastic contribution*. There are two mechanisms for such resonances; if the "force" in an inelastic channel is strong enough to support a bound state in the absence of the coupling between the elastic and inelastic channels, then the bound state will appear as a resonance in the elastic channel when the coupling between the two channels is "turned on." This mechanism has been invoked to explain the $\pi\Lambda$ resonance as a bound state of the $\bar{K}N$ channel by Dalitz,[5] and has been investigated in detail in a static model by Lee and Klein.[6] Sakurai[7] has suggested that the same mechanism may perhaps account for the higher resonances—in this case, bound states of the ρN channel.

The second, and perhaps less well known, mechanism is operative when there is a strong coupling between the elastic channel and an inelastic channel. Even below the threshold of the inelastic process, the system can make a transition to the inelastic channel, virtually. When the coupling is strong, the system can "oscillate" strongly between the two channels and tends to stay in this relatively stable configuration, developing a resonance. It is this picture that we wish to propose as the mechanism for the higher resonances in pion-nucleon scattering. The same mechanism has been discussed by Blankenbacler[8] to account for the two-pion resonance (ρ meson) in terms of the three-pion resonance (ω meson).

In the next section, we shall present a more detailed and precise description of the model we will consider. Briefly, this model may be summarized as follows: The higher resonances in pion-nucleon scattering are caused by a strong coupling between the pion-nucleon channel and the ρ meson (resonating two pions)-nucleon channel. As a guide to the nature of the coupling of these two channels, the one-pion exchange (OPE) diagram of the process $\pi+N\to\pi+\pi+N$ is studied. The analyticity of the helicity–angular-momentum projections of the OPE amplitude is investigated, and a pole approximation to the projection of the OPE amplitude is described (Sec. II).

In Sec. III the coupled equations resulting from the approximations presented in Sec. II are solved, and their analyticity and structure are discussed. Also in Sec. III explicit calculations are presented for $D_{\frac{3}{2}}$ and $F_{\frac{5}{2}}$ waves. In the conclusions we compare this calculation to other models which have been proposed recently.

* Supported in part by the Air Force Office of Scientific Research, Air Research and Development Command.

† Research supported in part by the United States Air Force under Grant No. AR-AFOSR-61-19 monitored by the Air Force Office of Scientific Research of the Air Research and Development Command.

‡ On leave of absence from the University of Pennsylvania, Philadelphia, Pennsylvania.

[1] L. F. Cook, Jr., and B. W. Lee, Phys. Rev. **127**, 283 (1962), hereafter referred to as I.

[2] See, e.g., J. M. Blatt and V. F. Weisskopf, *Theoretical Nuclear Physics* (J. Wiley & Sons, New York, 1952), Chap. VIII to X.

[3] J. S. Ball and W. R. Frazer, Phys. Rev. Letters **7**, 204 (1961).

[4] M. Nauenberg and A. Pais (to be published).

[5] R. Dalitz, Phys. Rev. Letters **6**, 239 (1961).

[6] B. W. Lee and A. Klein, Nuovo cimento **13**, 891 (1959).

[7] J. J. Sakurai, Phys. Rev. Letters **7**, 355 (1961).

[8] R. Blankenbecler (to be published).

II. ANALYTICITY OF THE MODEL

A. Physical Approximation

Our goal in this paper is to determine the three amplitudes M_{22}, M_{23} (M_{32}), and M_{33}, as they are defined in I, when they are coupled through the constraints imposed by the unitarity relations. The contribution of the production process to the elastic scattering is expected to be important in the region of the second and third resonances, roughly from 500 MeV to 900 MeV, where the production cross section becomes sizable. Therefore the coupled-channel problem will be mainly of interest in this energy region.

As in the previous paper, we shall truncate the unitarity relations at the three-particle states, in order to obtain a closed problem and hope that the solution will approximate reality, at least in the energy region considered.

In this energy region, higher angular momentum states than s and p are excited, and the statistical weights[9] attached to higher angular momentum states make their contributions to the cross section more important than those from s and p states. Recent work on the high-energy limit of the two-particle scattering amplitude[10] indicates that the s- and p-wave amplitudes require *ad hoc* parameters (subtractions in the dispersion relation), and we expect that the behavior of the $S_{\frac{1}{2}}$- and $P_{\frac{1}{2}}$-wave phase shifts will be influenced significantly by these parameters. Experimentally, the $D_{\frac{3}{2}}^{(\frac{1}{2})}$ and $F_{\frac{5}{2}}^{(\frac{1}{2})}$ states are known to dominate the second and third resonances.[11] Therefore, we shall concentrate our attention to these two angular momentum states.

Since we know very little about the analytic structure of production amplitudes and the three-particle scattering amplitude, we will eventually have to rely on a model. We assume that the scattering in the $D_{\frac{3}{2}}$ and $F_{\frac{5}{2}}$ states is driven mainly by the inelastic processes. This is partly supported by the experimental fact that, for energies up to and slightly above the (3,3) resonance, these phase shifts are small.[12] This means that the resonance behavior of the $D_{\frac{3}{2}}$ and $F_{\frac{5}{2}}$ phase shifts is essentially independent of the left-hand cuts of these partial-wave amplitudes. We shall therefore completely neglect the left-hand singularities of the elastic amplitudes in these angular-momentum states. Cini and Fubini[13] considered these phase shifts within the framework of their approximate version of the Mandelstam representation. While the low-energy behavior of these phase shifts may be controlled by the nearby left-hand singularities, it is clear that the resonance behavior cannot possibly depend on these singularities.

In the final state of the production process, $N+\pi \to N+\pi+\pi$, we assume that only the pions interact strongly. We are of course well aware of the overwhelming experimental evidences[14] for the isobar correlation of the final nucleon and a pion, but we would like to take, in the present work, the point of view that the higher resonances are not caused primarily by the (3,3) isobar in the final state. The angular distribution, polarization, etc., of the production are sensitive to the formation of the (3,3) isobar in the final state, but we shall not concern ourselves with these aspects of the problem.

The left-hand cuts of M_{33} will be completely neglected: it is consistent with the assumption that only the pion pair interact in the three-particle state. We recall from I that the disconnected graph, in which the nucleon is noninteracting and only the pions interact as a pair, is excluded from M_{33}. In this picture, the three-particle scattering process is also driven by the coupling of the two- and three- particle channels.

We assume that the two pions in the final state of the process $\pi+N \to \pi+\pi+N$ are produced only in the $T=J=1$ state. Since these pions are assumed to be strongly interacting, the two-pion state may be considered as an unstable vector boson[15] in all kinematical considerations. Following the convention we shall refer to this system as ρ meson. More specifically, it is a two-pion system with spin 1, parity -1, isotopic spin 1, and a mass distribution centered at $\simeq 5.4\ \mu$.[16] Since the ρ meson has spin 1 and negative parity, the orbital angular momentum of the ρN system is in general different from that of the πN system for given J and II. The orbital angular momentum of the ρN system corresponding to the angular momentum of the πN system, L_J, is tabulated in Table I.

The production amplitude M_{32} may be written, as

TABLE I. The angular momentum states of the ρ-N system, I_J, corresponding to the angular momentum states of the π-N system, L_J.

πN system L_J	ρN system I_J
$S_{\frac{1}{2}}$	$S_{\frac{1}{2}}$, $D_{\frac{1}{2}}$
$P_{\frac{3}{2}}$	$P_{\frac{3}{2}}$
$P_{\frac{1}{2}}$	$P_{\frac{1}{2}}$, $F_{\frac{5}{2}}$
$D_{\frac{3}{2}}$	$S_{\frac{3}{2}}$, $D_{\frac{3}{2}}$
$D_{\frac{5}{2}}$	$D_{\frac{5}{2}}$, $G_{\frac{7}{2}}$
$F_{\frac{5}{2}}$	$P_{\frac{3}{2}}$, $F_{\frac{5}{2}}$

[9] To be more specific, we mean the factor $(2j+1)$.

[10] M. Froissart, Phys. Rev. **123**, 1054 (1961); O. W. Greenberg and F. E. Low (to be published); V. Singh and B. M. Udgaonkar, *ibid.* **123**, 1487 (1961).

[11] B. Moyer, Revs. Modern Phys. **33**, 367 (1961).

[12] W. D. Walker, J. Davis and J. D. Shepherd, Phys. Rev. **118**, 1612 (1960).

[13] M. Cini and S. Fubini, *Proceedings of the 1960 Annual International Conference on High-Energy Physics at Rochester* (Interscience Publishers, Inc., New York, *1960*), p. 310; J. Bowcock, N. Cottingham, and D. Lurié, Nuovo cimento **19**, 142 (1961).

[14] An extensive bibliography may be found in R. M. Sternheimer and S. J. Lindenbaum, Phys. Rev. **123**, 333 (1961).

[15] B. W. Lee and M. T. Vaughn, Phys. Rev. Letters **4**, 578 (1960); P. Carruthers, Ann. Phys. (New York) **14**, 229 (1961).

[16] A. Erwin, R. March, W. D. Walker and E. West, Phys. Rev. Letters **6**, 628 (1961).

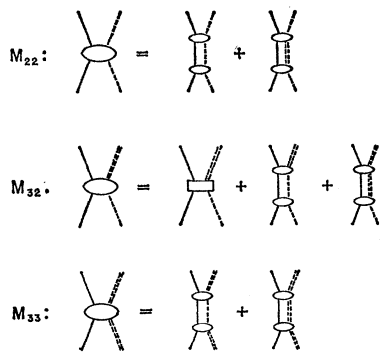

FIG. 1. A schematic representation of the analyticity chosen for the coupled channels. The square represents left-hand singularities.

in I,

$$M_{32}{}^{J\text{II}}(s,\sigma)=[g_3{}^I(w,\sigma)]^{\frac{1}{2}}F_{32}{}^J(w,\sigma)[g_2{}^L(w)]^{\frac{1}{2}}.$$

We suppress l, $l=1$ being understood hereafter. As we shall show, the factor $g_3{}^I(w,\sigma)$ removes the zero of $M_{32}{}^{J\text{II}}$ at $w=m+\sqrt{\sigma}$, so that $F_{32}{}^{J\text{II}}$ is finite at the production threshold. Therefore, the energy variation of $M_{32}{}^{J\text{II}}$ near the production threshold is given by the energy dependence of the factor $g_3{}^I(w,\sigma)$:

$$[g_3{}^I(w,\sigma)]^{\frac{1}{2}}\propto[Q(w,\sigma)]^{I+\frac{1}{2}}.$$

That is to say, the energy variation (power law) of the production amplitude near the production threshold is given by the centripetal barrier effect. Therefore, the s wave in the final ρN channel gets excited first, then the p wave, and so forth. Correspondingly, we expect the effect of the opening of the ρN channel to manifest itself first in the $D_{\frac{3}{2}}$, $S_{\frac{1}{2}}$ states, then in the $F_{\frac{5}{2}}$, $P_{\frac{3}{2}}$, $P_{\frac{1}{2}}$ states, etc., in the πN channel (refer to Table I). This corresponds to the ordering of the higher resonances in the $T=\frac{1}{2}$ channel, which are known experimentally to be $D_{\frac{3}{2}}$ and $F_{\frac{5}{2}}$.[11]

Recently, vector mesons of negative G parity (which decay into 3π) have been discovered[17] ($\eta^0\sim4\mu$, $\omega^0\sim5.6\mu$). There is reason to believe, however, that these mesons are not so important as the ρ meson in explaining the higher resonances. The reason is that, in order for the process $\pi+N\rightarrow\eta^0(\omega^0)+N$ to proceed, at least two pions must be exchanged between the nucleon and the meson, and the range of the force associated with this process is shorter than that associated with the production of the ρ meson, so that the primary effect is likely to show up mainly in low angular momentum states (s and p, say).

To recapitulate: Speaking loosely, since all amplitudes are coupled to one another through unitarity, the scheme employed here considers M_{22} and M_{33} to be driven by M_{23} through unitarity, while M_{23} itself is driven by its source (left-hand singularities). The model assumed is schematically pictured in Fig. 1, and this figure summarizes the physical content of the model.

[17] B. C. Maglić, L. W. Alvarez, A. H. Rosenfeld and M. L. Stevenson, Phys. Rev. Letters **7**, 192 (1961); N. H. Xuong and G. R. Lynch, *ibid.* **7**, 327 (1961).

B. One-Pion Exchange Approximation

Given the left-hand discontinuity of M_{23}, it could be substituted into Eq. (I39) to determine the N's and thus the amplitudes in the spirit of the model given in Sec. II A. However, these discontinuities of M_{23} are not known in any detail, and even if they were, it is not at all clear that the resulting coupled system could be solved by a practical calculation. Thus, we will choose a specific left-hand discontinuity which can be calculated from the Cutkosky diagram and has relatively simple properties. In order to insure that the contribution of this singularity to the production amplitude is significant, we impose the condition that this singularity be close to the physical region. Such a discontinuity is given by the OPE diagram shown in Fig. 2.

Referring to I we see that the singularities arising from this diagram are near the physical region. Using the same notation as I, the branch point is a function of σ in the w plane. As σ is increased, the branch point moves to the right until it reaches $w=m+\mu$. It then circles $w=m+\mu$ (by use of the $i\epsilon$) and moves to the left until $\sigma=4\mu^2$. When $\sigma>4\mu^2$, the branch point becomes complex, see I, Fig. 4. The OPE diagram thus dominates the nonphysical region, $w_2\leq w\leq w_3$, of the production amplitude.

Instead of the definition given in I, it is more convenient to define M_{23} and M_{32} as

$$\begin{aligned}M_{23}&=i\langle k,p(\text{out})\,|\,f^\dagger\,|\,k_1,k_2(\text{in})\rangle u(q)\\&\qquad\times[2k_02k_{10}2k_{20}p_0/m]^{\frac{1}{2}},\\M_{32}&=-i\bar{u}(q)\langle k_1,k_2(\text{out})\,|\,f\,|\,k,p(\text{in})\rangle\\&\qquad\times[2k_{10}2k_{20}2k_0p_0/m]^{\frac{1}{2}},\end{aligned}\tag{1}$$

in order to discuss the effects of the OPE diagram. The new definition is adopted so that the OPE terms of M_{23} and M_{32} are real in the physical region. One can convince himself by inspection that the unitarity condition, Eq. (I5), is not altered by this new definition of the amplitudes, nor is the relation between them.

Let us denote by B_{23} and B_{32} the OPE amplitudes of M_{23} and M_{32}. One can readily show that

$$\begin{aligned}B_{23}&=g\bar{u}(p)\gamma_5u(q)(t-\mu^2)^{-1}\langle k\,|\,j_\pi\,|\,k_1,k_2(\text{in})\rangle,\\B_{32}&=-g\bar{u}(q)\gamma_5u(p)(t-\mu^2)^{-1}\langle k_1,k_2(\text{out})\,|\,j_\pi{}^\dagger\,|\,k\rangle,\end{aligned}\tag{2}$$

where $t=-(p-q)^2$, g is the πN coupling constant such that $g/4\pi\approx14$, j_π is the pion current operator and, further,

$$[\bar{u}(p)\gamma_5u(q)]^*=-\bar{u}(q)\gamma_5u(p).\tag{3}$$

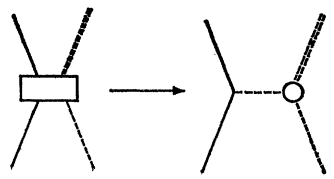

FIG. 2. The specific diagram (OPE) which approximates the left-hand discontinuities of M_{32}.

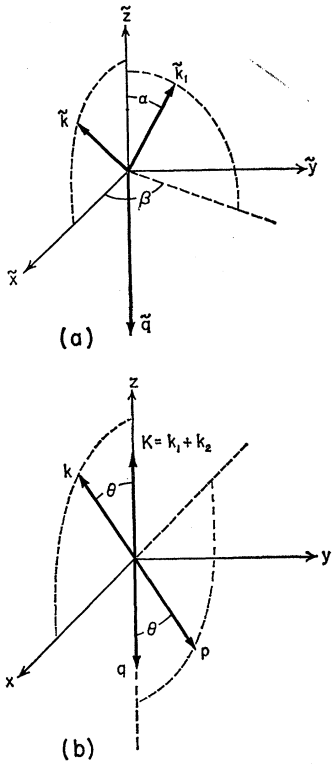

FIG. 3. The coordinate systems and vectors relevant to a discussion of a three-particle system. (a) is in the c.m. of the two pions; (b) is in the c.m. of the three-particle system. The tilde notation is the same as the prime.

We have suppressed, for the moment, the isotopic spin dependence.

Let us concentrate on the decomposition of B_{32}. In analogy to Eq. (I15), we have, with $\rho=\sigma^{\frac{1}{2}}$,

$$\langle\nu,\lambda|B_{32}{}^{Jl}(w,\rho)|\lambda\rangle$$
$$=2\pi\int d\Xi\, Y_{l\Lambda}{}^*(\alpha,\beta)\int_{-1}^{1} d(\cos\theta)\, d^J{}_{\Lambda-\nu,-\lambda}(\theta)$$
$$\times B_{32}[s,\sigma,\Phi=0,\Xi,\Omega=(\theta,0);\nu,\lambda]. \quad (4)$$

Since, in the integrand of Eq. (4), we require the OPE amplitude for $\gamma=0$, the rotation operator, $R_{\delta,\gamma,-\delta}$, in I [Sec. III B] is $R_{\delta,0,-\delta}=1$, so that the C' frame and the C frame are connected by a pure Lorentz transformation, Z. Consequently, the vector $\mathbf{k}_c$ lies in the $\mathbf{x}_c\mathbf{z}_c$ plane (see Fig. 3).

TABLE II. The linearly independent combinations of helicity amplitudes with definite parity.

$\langle\nu,\Lambda\|B_{32}{}^J\|\lambda\rangle\pm\langle-\nu,-\Lambda\|B_{32}{}^J\|\lambda\rangle$	Orbital parity	ζ
$\langle+,+1\|B^J\|+\rangle+\langle-,-1\|B^J\|+\rangle$	$(-1)^{J+\frac{1}{2}}$	1
$\langle+,+1\|B^J\|+\rangle-\langle-,-1\|B^J\|+\rangle$	$(-1)^{J-\frac{1}{2}}$	2
$\langle+,0\|B^J\|+\rangle+\langle-,0\|B^J\|+\rangle$	$(-1)^{J+\frac{1}{2}}$	3
$\langle+,0\|B^J\|+\rangle-\langle-,0\|B^J\|+\rangle$	$(-1)^{J-\frac{1}{2}}$	4
$\langle+,-1\|B^J\|+\rangle+\langle-,+1\|B^J\|+\rangle$	$(-1)^{J+\frac{1}{2}}$	5
$\langle+,-1\|B^J\|+\rangle-\langle-,+1\|B^J\|+\rangle$	$(-1)^{J-\frac{1}{2}}$	6

If we reduce $\bar{u}(p)\gamma_5 u(q)$ into the Pauli representation and pick out the states of definite helicity, we obtain $[(+)=\frac{1}{2},(-)=-\frac{1}{2}]$

$$\bar{u}_\pm(p)\gamma_5 u_+(q)=\left[\frac{E+m}{2m}\left(\frac{Q_0+m}{2m}\right)\right]^{\frac{1}{2}}$$
$$\times\left[\frac{P(s)}{E+m}\mp\frac{Q(s,\sigma)}{Q_0+m}\right]\begin{bmatrix}\cos\\ \sin\end{bmatrix}(\tfrac{1}{2}\theta), \quad (5)$$

where $\cos\theta=\hat{p}\cdot\hat{q}$ in the total c.m. system, and

$$|\mathbf{p}|=|\mathbf{k}|=P(s),$$
$$|\mathbf{q}|=|\mathbf{K}|=Q(s,\sigma), \quad (6)$$
$$p_0=E,\quad q_0=Q_0.$$

As we have stated, we assume that $\pi-\pi$ scattering is dominated by the $J=T=1$ state, so that[18]

$$\langle k_1,k_2(\text{out})|j_\pi|k\rangle\simeq-16\pi\sqrt{2}(\rho^2/\rho^2-4\mu^2)^{\frac{1}{2}}$$
$$\times e^{i\delta_1}\sin\delta_1\times 3(2k\cdot(k_1-k_2)/\rho^2-4\mu^2), \quad (7)$$

where $\rho^2=\sigma$, and δ_1 is the $\pi\pi$ phase shift in the $T=J=1$ state. Now in the two-pion c.m. system, we can write[19] [see Fig. 3(a)]

$$\tfrac{1}{2}(k_1-k_2)\cdot k=(\tfrac{1}{4}\rho)[(t-\rho^2-\mu^2)^2-4\rho^2\mu^2]^{\frac{1}{2}}(\rho^2-4\mu^2)^{\frac{1}{2}}\frac{4\pi}{3}\sum_{\Lambda=0,\pm1}Y_{1\Lambda}(\alpha,\beta)Y_{1\Lambda}{}^*(\pi-\chi,0), \quad (8)$$

where $\cos\chi=\hat{k}\cdot\hat{q}$, so that

$$\langle\nu,\Lambda|B_{32}{}^{TJ}(w,\rho)|\lambda\rangle=2\pi\begin{Bmatrix}\sqrt{2}\\ 1/\sqrt{2}\end{Bmatrix}\int_{-1}^{1} d\cos\theta\, d_{\nu-\Lambda,\lambda}{}^J(\theta)g\bar{u}_\nu(q)\gamma_5 u_\lambda(p)\frac{1}{t-\mu^2}4\pi\frac{[(t-\rho^2-\mu^2)^2-4\rho^2\mu^2]^{\frac{1}{2}}}{\rho(\rho^2-4\mu^2)^{\frac{1}{2}}}Y_{1,-\Lambda}{}^*(\chi,0)$$
$$\times\{-16\sqrt{2}\pi[\rho^2/(\rho^2-4\mu^2)]^{\frac{1}{2}}e^{i\delta_1}\sin\delta_1\},\quad\text{for}\quad T=\begin{Bmatrix}\frac{1}{2}\\ \frac{3}{2}\end{Bmatrix}. \quad (9)$$

Since

$$\cos\chi=\hat{k}_{1c}\cdot\hat{q}_c=\left[Q\frac{w^2-m^2+\mu^2}{2w\rho}-P\frac{w^2-m^2+\rho^2}{2w\rho}z\right]\frac{2\rho}{[(t-\mu^2-\rho^2)^2-4\rho^2\mu^2]^{\frac{1}{2}}},$$
$$\sin\chi=P(1-z^2)^{\frac{1}{2}}2\rho/[(t-\rho^2-\mu^2)^2-4\rho^2\mu^2]^{\frac{1}{2}},$$

[18] The normalization of the asymptotic state $|k_1,k_2(\ )\rangle$ is such that
$$|k_1,k_2(\ )\rangle=(1/\sqrt{2})a^{\dagger(\ )}(k_1)a^{\dagger(\ )}(k_2)|\text{vac}\rangle.$$

[19] We have $Y_{1,\pm1}(\theta,\phi)=\mp\frac{1}{2}(3/2\pi)^{\frac{1}{2}}\sin\theta e^{\pm i\phi}$, $Y_{1,0}(\theta,\phi)=\frac{1}{2}(3/\pi)^{\frac{1}{2}}\times\cos\theta$; c.f., A. R. Edmonds, *Angular Momentum in Quantum Mechanics* (Princeton University Press, Princeton, New Jersey, 1957).

where $z=\cos\theta$, we may rewrite Eq. (9) as

$$\langle\nu,\Lambda|B_{32}{}^{TJ}(w,\rho)|\lambda\rangle=\begin{Bmatrix}2\\1\end{Bmatrix}\left[-48\pi\frac{\rho}{\rho^2-4\mu^2}e^{i\delta_1}\sin\delta_1\right]\left(\frac{8\pi}{3}\right)g2\pi\int_{-1}^{1}dz\,d_{\nu-\Lambda,\lambda}{}^{J}(\theta)\bar{u}_\nu(q)\gamma_5 u_\lambda(p)\frac{1}{t-\mu^2}$$
$$\times\begin{bmatrix}+P(1-z^2)^{\frac{1}{2}}\\ \sqrt{2}\{Q(w^2-m^2+\mu^2)/2w\rho-P[(w^2-m^2+\rho^2)/2w\rho]z\}\\ -P(1-z^2)^{\frac{1}{2}}\end{bmatrix},\quad\text{for}\quad\Lambda=\begin{bmatrix}1\\0\\-1\end{bmatrix}. \tag{10}$$

As pointed out in I, it is more convenient to form linear combinations of the amplitudes such that eigenfunctions of parity are obtained. The six, so formed, linearly independent amplitudes are given in Table II. They are labeled by ζ rather than ξ (as in I) for a more explicit identification.

Defining $B_{32}{}^{J}$, with T suppressed, as

$$B_{32}{}^{J\zeta}(w,\rho)\equiv\langle\nu,\Lambda|B_{32}{}^{J}|\lambda\rangle\pm\langle-\nu,-\Lambda|B_{32}{}^{J}|\lambda\rangle,$$

and using Eq. (10) with Table II, we can write

$$B_{32}{}^{TJ\zeta}=\begin{Bmatrix}2\\1\end{Bmatrix}\left[-48\pi\frac{\rho}{\rho^2-4\mu^2}e^{i\delta_1}\sin\delta_1\right]\left(\frac{8\pi}{3}\right)^{\frac{1}{2}}g2\pi\int_{-1}^{1}dz\,P^{J\zeta}(z)\frac{1}{t-\mu^2}\left[\frac{E+m}{2m}\left(\frac{Q_0+m}{2m}\right)\right]^{\frac{1}{2}}, \tag{11}$$

where ($l=J-\frac{1}{2}$ in the following expressions)

$$P^{J1}(z)=P(1-z^2)^{\frac{1}{2}}\left[\left(-\frac{Q}{Q_0+m}+\frac{P}{E+m}\right)\cos\tfrac{1}{2}\theta d_{-\frac{1}{2},\frac{1}{2}}{}^{J}(\theta)-\left(\frac{Q}{Q_0+m}+\frac{P}{E+m}\right)\sin\tfrac{1}{2}\theta d_{\frac{1}{2},\frac{1}{2}}{}^{J}(\theta)\right]$$
$$=-\frac{P(1-z^2)}{l+1}\left[\frac{Q}{Q_0+m}P_{l+1}{}'(z)-\frac{P}{E+m}P_l{}'(z)\right],$$
$$P^{J2}(z)=-\frac{P(1-z^2)}{l+1}\left[\frac{Q}{Q_0+m}P_l{}'(z)-\frac{P}{E+m}P_{l+1}{}'(z)\right],$$
$$P^{J3}(z)=\sqrt{2}\left[Q\frac{w^2-m^2+\mu^2}{2w\rho}-P\frac{w^2-m^2+\rho^2}{2w\rho}z\right]\left[-\frac{Q}{Q_0+m}P_{l+1}(z)+\frac{P}{E+m}P_l(z)\right], \tag{12}$$
$$P^{J4}(z)=\sqrt{2}\left[Q\frac{w^2+m^2+\mu^2}{2w\rho}-P\frac{w^2-m^2+\rho^2}{2w\rho}z\right]\left[-\frac{Q}{Q_0+m}P_l(z)+\frac{P}{E+m}P_{l+1}(z)\right],$$
$$P^{J5}(z)=-\frac{P(1-z^2)}{l+1}\left[\frac{Q}{Q_0+m}\left(\frac{l}{l+2}\right)^{\frac{1}{2}}P_{l+1}{}'(z)-\frac{P}{E+m}\left(\frac{l+2}{l}\right)^{\frac{1}{2}}P_l{}'(z)\right],$$
$$P^{J6}(z)=-\frac{P(1-z^2)}{l+1}\left[\frac{Q}{Q_0+m}\left(\frac{l+2}{l}\right)^{\frac{1}{2}}P_l{}'(z)-\frac{P}{E+m}\left(\frac{l}{l+2}\right)P_{l+1}{}'(z)\right].$$

As Table II shows, the parity eigen amplitudes naturally separate into two groups. A πN system in one of the states, $P_{\frac{1}{2}}$, $D_{\frac{3}{2}}$ or $F_{\frac{5}{2}}$, can produce a $(\pi\pi)N$ state with appropriate J and T and $\zeta=1$, 3, 5, but not $\zeta=2$, 4, 6. On the other hand, the states $S_{\frac{1}{2}}$, $P_{\frac{3}{2}}$ are characterized by $\zeta=2$, 4, 6, and not by $\zeta=1$, 3, 5. Incidentally, in the description of the $\pi\pi$ system as an unstable vector boson, the states $\zeta=1$, 2, 5, 6, correspond to the longitudinal polarization of the vector boson, while the states $\zeta=3$, 4, correspond to the transverse polarization.

As in I, we define new amplitudes $F_{22}{}^{J\text{II}}(w)$, $F_{23}{}^{J\zeta}(w,\rho)$, $F_{32}{}^{J\zeta}(w,\rho)$ and $F_{33}{}^{J\zeta\zeta'}(w,\rho,\rho')$, which are free of kinematical singularities, by

$$F_{22}{}^{J\text{II}}(w)=g_2{}^{L}(w)M_{22}{}^{J\text{II}}(w),$$
$$F_{23}{}^{J\zeta}(w,\rho)=[g_2{}^{L}(w)g_3{}^{I}(w,\rho)]^{\frac{1}{2}}M_{23}{}^{J\zeta}(w,\rho),$$
$$F_{23}{}^{J\zeta}(w-i\epsilon,\rho-i\eta)=[F_{32}{}^{J\zeta}(w+i\epsilon,\rho+i\eta)]^{*}, \tag{13}$$
$$F_{33}{}^{J\zeta\zeta'}(w,\rho,\rho')=[g_3{}^{I}(w,\rho)]^{\frac{1}{2}}M_{33}{}^{J\zeta\zeta'}(w,\rho,\rho')\times[g_3{}^{I'}(w,\rho')]^{\frac{1}{2}}.$$

In Eq. (13), we have

$$g_2{}^L(w)=\frac{2m}{E+m}\left(\frac{E+m}{P}\right)^{2L}, \tag{14}$$

where L is the orbital angular momentum of the πN system in the state (J,II), and

$$g_3{}^I(w,\rho)=\frac{2m}{Q_0+m}\left(\frac{Q_0+m}{Q}\right)^{2I}, \tag{15}$$

where is the lowest orbital angular momentum of the $(\pi\pi)_{l=1}N$ system in the state (J,ζ). Of course, the phase space densities are modified as in (I35)

$$\rho_2{}^L(w)=\frac{1}{4(2\pi)^3}\frac{P^{2L+1}}{w}\frac{1}{(E+m)^{2L+1}}\theta(w-(m+\mu)),$$

$$\rho_3{}^I(w,\rho)d\rho=\frac{1}{8(2\pi)^6}\frac{Q^{2I+1}}{2w}\frac{1}{(Q_0+m)^{2I-1}}\rho d\rho\left[\frac{\rho^2-4\mu^2}{\rho^2}\right]^{\frac{1}{2}}$$
$$\times\theta(\rho-2\mu)\theta(w-m-\rho). \tag{16}$$

Finally, we obtain the discontinuity of F_{32} along its left-hand cut, due to the OPE diagram, as

$$[\text{disc}F_{32}{}^{TJ}(w,\rho)]_L=\text{disc}\left[\left(\frac{2m}{E+m}\right)^{\frac{1}{2}}\left(\frac{2m}{Q_0+m}\right)^{\frac{1}{2}}\left(\frac{E+m}{P}\right)^{L}\left(\frac{Q_0+m}{Q}\right)^{I}B_{32}{}^{TJ\zeta}(w,\rho)\right]$$
$$=\begin{Bmatrix}2\\1\end{Bmatrix}\left(-48\pi\frac{\rho}{\rho^2-4\mu^2}e^{i\delta_1}\sin\delta_1\right)\left(\frac{8\pi}{3}\right)^{\frac{1}{2}}g2\pi\,\text{disc}\left[\left(\frac{E+m}{P}\right)^{L}\left(\frac{Q_0+m}{Q}\right)^{I}\int_{-1}^{1}dz\,P^{J\zeta}(z)\frac{1}{t-\mu^2}\right]. \tag{17}$$

The w dependence of the left-hand-cut contribution to $F_{32}{}^{TJ}$ comes entirely from

$$I^{J\zeta}=\left(\frac{E+m}{P}\right)^{L}\left(\frac{Q_0+m}{Q}\right)^{I}\int_{-1}^{1}dz\,P^{J\zeta}(z)\frac{1}{t-\mu^2}. \tag{18}$$

Let us study this function for $\zeta=1$, 3, and 5, which are proper for the $D_{\frac{3}{2}}$ and $F_{\frac{5}{2}}$ states of the πN system.

Longitudinal:

$$I^{J1}=-\frac{1}{Q}\left(\frac{E+m}{P}\right)^{L}\left(\frac{Q_0+m}{Q}\right)^{I}\left\{\frac{P}{E+m}\frac{l}{2l+1}[Q_{l-1}(x)-Q_{l+1}(x)]-\frac{Q}{Q_0+m}\frac{l+2}{2l+3}[Q_l(x)-Q_{l+2}(x)]\right\},$$
$$I^{J5}=-\frac{1}{Q}\left(\frac{E+m}{P}\right)^{L}\left(\frac{Q_0+m}{Q}\right)^{\frac{1}{2}}[l(l+2)]^{\frac{1}{2}}\left\{\frac{Q}{Q_0+m}\frac{1}{2l+3}[Q_l(x)-Q_{l+2}(x)]-\frac{P}{E+m}\frac{1}{2l+1}[Q_{l-1}(x)-Q_{l+1}(x)]\right\}; \tag{19}$$

Transverse:

$$I^{J3}=-\frac{1}{PQ}\left(\frac{E+m}{P}\right)^{L}\left(\frac{Q_0+m}{Q}\right)^{I}\sqrt{2}\left\{Q\frac{w^2-m^2+\mu^2}{2w\rho}\left[-\frac{Q}{Q_0+m}Q_{l+1}(z)+\frac{P}{E+m}Q_l(x)\right]\right.$$
$$\left.+P\frac{w^2-m^2+\rho^2}{2w\rho}\left[\frac{P}{E+m}\frac{1}{2l+1}[(l+1)Q_{l+1}(x)+lQ_{l-1}(x)]-\frac{Q}{Q_0+m}\frac{1}{2l+3}[(l+2)Q_{l+2}(x)+(l+1)Q_l(x)]\right]\right\};$$

where $Q_l(x)$ is the Legendre function of the second kind,

$$l=J-\tfrac{1}{2},\quad x=(2EQ_0-2m^2+\mu^2)/2PQ. \tag{20}$$

We note: (1) The branch cut of $Q_l(x)$ for $\rho^2>2\mu^2\times(1+\mu/2m)$ must be defined in the manner prescribed in I, Sec. V. (2) Recalling that $I=0$, 1 for the $D_{\frac{3}{2}}$, $F_{\frac{5}{2}}$ states, and

$$\lim_{x\to\infty}Q_l(x)=\frac{l!}{(2l+1)!!}\left(\frac{1}{x}\right)^{l+1},\quad (l\text{ integer})$$

we deduce that $I^{J\zeta}$ and therefore $B^{J\zeta}$ are finite as $Q\to 0$. This proves the threshold behavior we have asserted. (3) Recalling that $Q_l(x)=(-1)^{l+1}Q_l(-x)$, we see that as w crosses the branch cuts of $P(s)$ or $Q(s,\sigma)$, $I^{J\zeta}(w,\rho)$ is continuous, i.e., $B^{J\zeta}$ is devoid of kinematical singularities. (4) As $w\to m+\mu$ along the real axis from $w>m+\mu$,

$$Q_l(x)\to -i(\pi/2)P_l(x),$$

since the branch cut described in (1) passes around $w=m+\mu$. Hence,

$$\lim_{w\to m+\mu}F_{32}{}^{J\zeta}(w,\rho)=\frac{\text{const}}{P^{2L+2}}.$$

Further consideration will convince the reader that the conclusions (2)–(4) are of general validity, holding

for all $B^{J\xi}$, and, secondly, that $B^{J\xi}(w,\sigma)$ is most singular at $w=m+\mu$.

This second remark leads to our last approximation. It is clear from Eq. (19) that the solution of the coupled equations, by use of Eq. (17), will be exceedingly complicated, and it seems quite likely that this complexity will obscure the physical results of our model. In order to avoid this difficulty we will replace the w dependence of $[\mathrm{disc}F_{32}{}^{TJ\xi}(w,\rho)]_L$ by a pole with appropriate position and residue.

Since $F_{32}(w,\rho)$ is most singular at $w=m+\mu=w_2$, it seems most reasonable to place the pole at that point so that

$$[\mathrm{disc}F_{32}{}^{TJ\xi}(w,\rho)]_L=\begin{Bmatrix}2\\1\end{Bmatrix}\left(-48\pi\frac{\rho}{\rho^2-4\mu^2}e^{i\delta_1}\sin\delta_1\right)\times\left(\frac{8\pi}{3}\right)^{\frac{1}{2}}2\pi g\Gamma^{J\xi}\pi\delta(w-w_2),\quad(21)$$

where the residue $\Gamma^{J\xi}$ must be determined.

In practice the method by which one determines $\Gamma^{J\xi}$ is not unique, and at least two procedures are possible. We may take $\Gamma^{J\xi}$ as a phenomenological parameter which can be varied to fit the data, or we may attempt to estimate its value by calculating the contributions from certain generalized perturbation theory diagrams. Since the validity of any calculation of a particular graph or set of graphs is uncertain, we prefer to use the first procedure, i.e., $\Gamma^{J\xi}$ is a parameter. However, we shall try to estimate the value of $\Gamma^{J\xi}$ from the OPE diagram in Sec. III C.

III. N/D EQUATIONS

A. Solution of the Coupled Equations

In this section we will solve the coupled N/D equations resulting from the physical approximations made in Sec. II. Rewriting Eq. (I36) for convenience, we have

$$N_{22}(w)=F_{22}(w)D_{22}(w)+\sum_{\xi''}\int d\rho''F_{23}{}^{\xi''}(w,\rho'')D_{32}{}^{\xi''}(w,\rho''),\quad(22a)$$

$$N_{23}{}^{\xi'}(w,\rho')=F_{22}(w)D_{23}{}^{\xi'}(w,\rho')+\sum_{\xi''}\int d\rho''F_{23}{}^{\xi''}(w,\rho'')D_{33}{}^{\xi''\xi'}(w,\rho'',\rho'),\quad(22b)$$

$$N_{32}{}^{\xi}(w,\rho)=F_{32}{}^{\xi}(w,\rho)D_{22}(w)+\sum_{\xi''}\int d\rho''F_{33}{}^{\xi\xi''}(w,\rho,\rho'')D_{32}{}^{\xi''}(w,\rho''),\quad(22c)$$

$$N_{33}{}^{\xi\xi'}(w,\rho,\rho')=F_{32}{}^{\xi}(w,\rho)D_{23}{}^{\xi'}(w,\rho')+\sum_{\xi''}\int d\rho''F_{33}{}^{\xi\xi''}(w,\rho,\rho'')D_{33}{}^{\xi''\xi'}(w,\rho'',\rho'),\quad(22d)$$

where we have suppressed the angular momentum and isotopic spin labels, and the N's and D's are defined as in I. The results of the previous section are implemented by imposing the boundary conditions

$$\begin{aligned}&[\mathrm{disc}F_{22}(w)]_L=0,\\&[\mathrm{disc}F_{32}{}^{\xi}(w,\rho)]_L=[\mathrm{disc}F_{23}{}^{\xi}(w,\rho)]_L{}^*\\&\qquad=\pi\Gamma^{\xi}f^T(\rho)\delta(w-w_2),\quad(23)\\&[\mathrm{disc}F_{33}{}^{\xi\xi'}(w,\rho,\rho')]_L=0,\end{aligned}$$

on Eq. (22), where $f^T(\rho)$ is defined as

$$f^T(\rho)=\begin{Bmatrix}2\\1\end{Bmatrix}\left(-48\pi\frac{\rho}{\rho^2-4\mu^2}e^{i\delta_1}\sin\delta_1\right)\left(\frac{8\pi}{3}\right)^{\frac{1}{2}}2\pi g,\quad\text{for}\quad T=\begin{Bmatrix}\frac{1}{2}\\\frac{3}{2}\end{Bmatrix}.\quad(24)$$

The isotopic spin label on $f^T(\rho)$ will usually be suppressed. The solutions of Eqs. (22) and (23), F_{ij}, will satisfy the unitarity relations, Eq. (I34), by construction, and further, since the discontinuities in Eq. (23) are symmetric, we are guaranteed that the F_{ij} will satisfy time-reversal invariance as well.

Taking the discontinuities of Eq. (24) and applying Cauchy's theorem to the N_{ij} we obtain

$$N_{22}(w)=\frac{1}{w_2-w}\sum_{\xi''}\Gamma^{\xi''*}\int d\rho''f^*(\rho'')D_{32}{}^{\xi''}(w_2,\rho''),\quad(25a)$$

$$N_{23}{}^{\xi'}(w,\rho')=\frac{1}{w_2-w}\sum_{\xi''}\Gamma^{\xi''*}\int d\rho''f^*(\rho'')D_{33}{}^{\xi''\xi'}(w_2,\rho'',\rho'),\quad(25b)$$

$$N_{32}{}^{\xi}(w,\rho)=\frac{1}{w_2-w}\Gamma^{\xi}f(\rho)D_{22}(w_2),\quad(25c)$$

$$N_{22}{}^{\xi\xi'}(w,\rho,\rho')=\frac{1}{w_2-w}\Gamma^{\xi}f(\rho)D_{23}{}^{\xi'}(w_2,\rho').\quad(25d)$$

The solutions of Eq. (25) are most conveniently expressed in terms of the following quantities

$$K_2{}^L(x,y)=\int_{w_2}^{\infty}dw'\,\frac{\rho_2{}^L(w')}{(w'-x)(w'-y)},\quad K_2{}^L(x,x)=K_2{}^L(x),\quad w_2=m+\mu;$$
$$G_3{}^I(x,y)=\sum_{\xi''}|\Gamma^{\xi''}|^2\int d\rho''|f(\rho'')|^2\int_{w_3}^{\infty}dw'\,\frac{\rho_3{}^I(w',\rho'')}{(w'-x)(w'-y)},\quad w_3=m+\rho'', \tag{26}$$
$$G_3{}^I(x,x)=G_3{}^I(x).$$

To solve for $N_{22}(w)$, for example, we substitute Eq. (25c) into the definition of $D_{32}(w,\rho)$ and replace $D_{32}(w_2,\rho'')$, in Eq. (25a), by the resulting expression. Eq. (25a) will involve $N_{22}(w)$ and $D_{22}(w_2)$; we express $D_{22}(w_2)$ in terms of $N_{22}(w)$, and obtain

$$N_{22}(w)=\frac{1}{w_2-w}G_3(w_2)-\frac{1}{w_2-w}G_3(w_2)\int_{w_2}^{\infty}dw'\,\frac{\rho_2(w')N_{22}(w')}{w'-w_2}, \tag{27}$$

where we have suppressed the angular momentum labels. Eq. (27) is a Fredholm equation of the second kind,[20] with *separable* kernel, and can be immediately solved for $N_{22}(w)$. This allows us to determine $D_{22}(w)$ and from Eq. (25c) we obtain $N_{32}(w,\rho)$ and then $D_{32}(w,\rho)$. Proceeding in a similar manner with Eq. (25b) and (25d), we obtain, using Eq. (26),

$$N_{22}(w)=-\frac{1}{w-w_2}\frac{G_3(w_2)}{1-K_2(w_2)G_3(w_2)},$$
$$N_{23}{}^{\xi}(w,\rho)=-\frac{1}{w-w_2}\Gamma^{\xi *}f^*(\rho)\frac{1}{1-K_2(w_2)G_3(w_2)},$$
$$N_{32}{}^{\xi}(w,\rho)=-\frac{1}{w-w_2}\Gamma^{\xi}f(\rho)\frac{1}{1-K_2(w_2)G_3(w_2)}, \tag{28}$$
$$N_{33}{}^{\xi\xi'}(w,\rho,\rho')=-\frac{1}{w-w_2}\Gamma^{\xi}\Gamma^{\xi' *}f(\rho)f^*(\rho')\frac{K_2(w_2)}{1-K_2(w_2)G_3(w_2)}.$$

These lead to

$$D_{22}(w)=1+K_2(w,w_2)G_3(w_2)/[1-K_2(w_2)G_3(w_2)],$$
$$D_{23}{}^{\xi}(w,\rho)=\Gamma^{\xi *}f^*(\rho)K_2(w,w_2)/[1-K_2(w_2)G_3(w_2)],$$
$$D_{32}{}^{\xi}(w,\rho)=\Gamma^{\xi}f(\rho)K_3(w,w_2;\rho)/[1-K_2(w_2)G_3(w_2)], \tag{29}$$
$$D_{33}{}^{\xi\xi'}(w,\rho,\rho')=\delta_{\xi\xi'}\delta(\rho-\rho')+\Gamma^{\xi}\Gamma^{\xi' *}f(\rho)f^*(\rho')K_2(w_2)K_3(w,w_2;\rho)/[1-K_2(w_2)G_3(w_2)],$$

where

$$K_3{}^I(x,y;\rho)=\int_{w_3}^{\infty}dw'\,\frac{\rho_3{}^I(w',\rho)}{(w'-x)(w'-y)}. \tag{30}$$

Returning to Eq. (23) it is a straight-forward computation to obtain the F_{ij}. One finds

$$F_{22}(w)=\frac{1}{w-w_2}\frac{G_3(w,w_2)-G_3(w_2)}{1-[K_2(w,w_2)-K_2(w_2)][G_3(w,w_2)-G_3(w_2)]},$$
$$F_{23}{}^{\xi}(w,\rho)=-\frac{\Gamma^{\xi *}f^*(\rho)}{G_3(w,w_2)-G_3(w_2)}F_{22}(w),$$
$$F_{32}{}^{\xi}(w,\rho)=[F_{23}{}^{\xi}(w^*,\rho^*)]^*, \tag{31}$$
$$F_{33}{}^{\xi\xi'}(w,\rho,\rho')=\Gamma^{\xi}\Gamma^{\xi' *}f(\rho)f^*(\rho')\frac{K_2(w,w_2)-K_2(w_2)}{G_3(w,w_2)-G_3(w_2)}F_{22}(w).$$

[20] E. T. Whittaker and G. N. Watson, *Course of Modern Analysis* (Cambridge University Press, New York, 1952), Chap. XI.

B. General Properties of the Solutions

One can easily show that the solutions in Eq. (31) satisfy the truncated unitarity condition, Eq. (I34). On the other hand, it appears that the original, assumed analyticity has been violated. Specifically, both $F_{22}(w)$ and $F_{33}(w,\rho,\rho')$ seem to have poles at $w=m+\mu$. Incidentally, if the delta function, $\delta(w-w_2)$, in $[\text{disc } F_{23}]_L$ had been chosen at some other point, say $w_0<w_2$, the structure of the solutions would be exactly the same, the only change being that w_2 is replaced by w_0 except when w_2 occurs as the lower limit of an integral. To show that F_{22} and F_{33} do not have poles at w_2, we refer to Eq. (26) and observe that

$$G_3{}^I(w,w_2)-G_3{}^I(w_2)$$
$$=(w-w_2)\sum_{\xi''}|\Gamma^{\xi''}|^2\int d\rho''\,|f(\rho'')|^2$$
$$\times\int_{w_3}^{\infty}dw'\,\frac{\rho_3{}^I(w',\rho'')}{(w'-w)(w'-w_2)^2} \tag{32}$$

and

$$K_2{}^L(w,w_2)=K_2{}^L(w_2)$$
$$=(w-w_2)\int_{w_2}^{\infty}dw'\,\frac{\rho_2{}^L(w')}{(w'-w)(w'-w_2)^2}.$$

Thus, in both F_{22} and F_{33} the pole singularity at w_2 cancels out. On the other hand, the pole at w_2 remains in F_{23} which is in agreement with Eq. (23).

To discuss the analyticity for $w>w_2$ it is more convenient to write $F_{22}(w)$ as

$$F_{22}(w)=-(w-w_2)^{-1}\{[K_2(w,w_2)-K_2(w_2)]$$
$$-[G_3(w,w_2)-G_3(w_2)]^{-1}\}^{-1}. \tag{33}$$

From Eqs. (26) and (33) we see that $F_{22}(w)$ is defined in a cut plane: an elastic cut coming from $K_2(w,w_2)$ and extending from w_2 to ∞, and an inelastic cut coming from $G_3(w,w_2)$ and extending from w_3 to ∞. Clearly, F_{23} and F_{33} are defined in planes cut in exactly the same manner, but, as seen from Eq. (31), with different discontinuities. As mentioned previously, these discontinuities are the proper ones to satisfy the truncated unitarity condition.

Before we proceed with a general discussion of the properties of the solutions in Eq. (31), it is convenient to introduce a nonessential approximation for the structure of the $\pi-\pi$ resonance. In particular, we write

$$e^{i\delta_1{}^{\pi\pi}}\sin\delta_1{}^{\pi\pi}\simeq\frac{(\gamma/2)[(\rho^2-4\mu^2)^3/\rho^2]^{\frac{1}{2}}}{\rho_R{}^2-\rho^2-i(\gamma/2)[(\rho^2-4\mu^2)^3/\rho^2]^{\frac{1}{2}}}.$$

Then in the limit of a narrow resonance

$$\sin^2\delta_1\to(\gamma/2)[(\rho^2-4\mu^2)^3/\rho^2]^{\frac{1}{2}}\pi\delta(\rho_R{}^2-\rho^2). \tag{34}$$

In these expansions, the half-width on a ρ scale, $\gamma_{\frac{1}{2}}$,

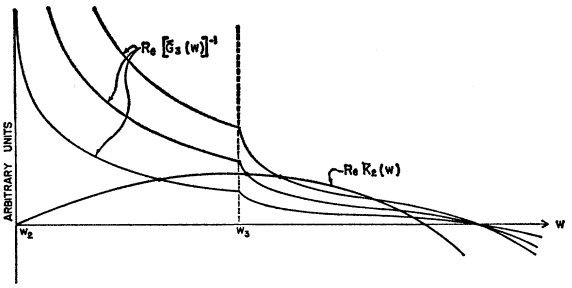

FIG. 4. A plot of $\mathrm{Re}\bar{K}_2(w)$ with three plots of $\mathrm{Re}[\bar{G}_3(w)]^{-1}$. The intersections between these two curves lead to resonances.

is given as

$$\gamma_{\frac{1}{2}}=(\gamma/4\rho_R)[(\rho_R{}^2-4\mu^2)^3/\rho_R{}^2]^{\frac{1}{2}},$$

with $\rho_R=5.4\mu$. This approximation will be used in the remainder of the paper, and its effects, which do not introduce any essential structural changes, will be discussed in a later section.

We are now in a position to discuss the general, physical properties of the solutions in Eq. (31) or (33). Consider the structure of $F_{22}(w)$. It is easy to see that the

$$\mathrm{Re}\{[K_2(w,w_2)-K_2(w_2)]-[G_3(w,w_2)-G_3(w_2)]^{-1}\}$$
$$\equiv\mathrm{Re}\{\bar{K}_2(w)-[\bar{G}_3(w)]^{-1}\}$$

can vanish, and thus produce a resonant behavior in $F_{22}(w)$. The "subtracted" forms, $\mathrm{Re}\bar{K}_2(w)$ and $\mathrm{Re}\bar{G}_3(w)$, are zero at $w=w_2$, and rise to a maximum before they pass through an appropriate zero point. However, we wish to compare $\mathrm{Re}[\bar{G}(w)]^{-1}$ with $\mathrm{Re}\bar{K}_2(w)$. From the remarks above, $\mathrm{Re}[\bar{G}_3(w)]^{-1}$ is infinite at w_2 and decreases as w is increased. Since $\bar{G}_3(w)$ develops an imaginary part when $w>w_3$, and the zero of $\mathrm{Re}\bar{G}_3(w)$ occurs for $w>w_3$, $\mathrm{Re}[\bar{G}_3(w)]^{-1}$ does not become infinite at the zero of $\mathrm{Re}[\bar{G}_3(w)]$, but passes through zero and becomes negative. Of course, $\mathrm{Re}\bar{G}_3(w)$ has a discontinuous slope at $w=w_3$, and so does $\mathrm{Re}[\bar{G}_3(w)]^{-1}$. Thus one may easily obtain the situation presented in Fig. 4. The curves in Fig. 4 do not represent the most general situation. In particular, the zeros may be interchanged so that there is only one intersection.

Several remarks can be made from Fig. 4:

(1) Two zeros can be obtained in the denominator of $F_{22}(w)$, and thus two resonances. However, the higher resonance probably has no significance at all. If the position of the higher resonance is much larger than w_3, then the effects of higher inelastic processes are undoubtedly important, and our solutions, subject to the constraints imposed by the *truncated* unitarity conditions, are no longer applicable. On the other hand, if such a resonance occurs near $w=w_3$, then it very well may be physically meaningful.

(2) For a given angular momentum state the curve of $\mathrm{Re}\bar{K}_2(w)$ is fixed, but the curve of $\mathrm{Re}[\bar{G}_3(w)]^{-1}$ need not be fixed. We have assumed that the $\pi-\pi$ cross

section is known from other sources, i.e., $f^T(\rho)$ is known, but we can still vary the parameter which characterizes the coupling between the elastic and inelastic channels, viz., $\Gamma^{J\zeta}$. If $\Gamma^{J\zeta}$ is increased then the entire $\mathrm{Re}[\bar{G}_3(w)]^{-1}$ curve is depressed, and vice versa. Three different values of $\Gamma^{J\zeta}$ are given on Fig. 4. This shows an important conclusion of the model presented here, viz., the position of the resonance is not necessarily above or below the inelastic threshold, contrary to Ball and Frazer,[3] but depends on the value of the parameter $\Gamma^{J\zeta}$. Incidentally, we do not need to know the phase of different ζ components of $\Gamma^{J\zeta}$ to determine $F_{22}(w)$ since only terms of the form $\sum_{\zeta''}|\Gamma^{\zeta''}|^2$ occur.

(3) It is important to realize, referring to the remarks just made, that $\Gamma^{J\zeta}$ cannot be varied at will to fit the data. Recalling the explicit form of $f^T(\rho)$, Eq. (24), we see that once $\Gamma^{J\zeta}$ and the $\pi-\pi$ cross section are fixed, the isotopic spin dependence is also determined. As an example, let us say that a resonance is present in the $D_{\frac{3}{2}}^{(\frac{1}{2})}\pi N$ system. Since the isotopic spin factors, in this model, occur as

$$\begin{Bmatrix}\frac{1}{2}\\ \frac{3}{2}\end{Bmatrix}\rightarrow\begin{Bmatrix}2\\ 1\end{Bmatrix}$$

and we need $|f^T|^2$, it follows that the $\bar{G}_3^{-1}$ curve for $T=\frac{3}{2}$ is increased by a factor of four over that for $T=\frac{1}{2}$. Thus we would expect the $D_{\frac{3}{2}}^{(\frac{3}{2})}$ system to exhibit a resonant behavior at higher values of w than the $D_{\frac{3}{2}}^{(\frac{1}{2})}$ state. We must emphasize that it is possible that the $\bar{G}_3^{-1}$ curve for $D_{\frac{3}{2}}^{(\frac{3}{2})}$ does not intersect the $\bar{K}_2$ curve, in which case there would be no resonant behavior. In fact, it could happen that neither the $D_{\frac{3}{2}}^{(\frac{1}{2})}$ or $D_{\frac{3}{2}}^{(\frac{3}{2})}$ states involve intersecting curves, and neither shows a resonance.

(4) It is clear from Eq. (31) that $F_{23}(w,\rho)$ and $F_{33}(w,\rho,\rho')$ will exhibit the same type of w dependence. In particular, if $F_{22}(w)$ exhibits a resonance, then $F_{23}(w,\rho)$ and $F_{33}(w,\rho,\rho')$ will also show a resonant behavior in w. Although the position and width of these resonances may be altered from that in $F_{22}(w)$, the general structure of the amplitudes will be the same since $\bar{K}_2$ and $\bar{G}_3$ are reasonably smooth functions. This point is quite relevant to the elastic and inelastic π-N scattering cross sections.

(5) Although there is no restriction as to whether a resonance will occur above or below the inelastic threshold, the magnitude of the elastic cross section will depend markedly on the position of the resonance relative to the inelastic threshold. Again consider the example of $D_{\frac{3}{2}}$. Let us say that $D_{\frac{3}{2}}^{(\frac{1}{2})}$ has a resonance for $w<w_3$, and $D_{\frac{3}{2}}^{(\frac{3}{2})}$ has a resonance for $w>w_3$. The magnitude of the $D_{\frac{3}{2}}^{(\frac{1}{2})}$ cross section will be much larger than that for $D_{\frac{3}{2}}^{(\frac{3}{2})}$. This may be seen as follows. Below w_3, the inelastic channel has no imaginary part, and the magnitude of the cross section at the resonance depends on only $\mathrm{Im}\bar{K}_2(w)$. However, above w_3, the magnitude of the cross section at resonance depends on the $\mathrm{Im}\bar{G}_3(w)$ as well. For $I=0$, 1 ($I=$lowest orbital angular momentum state in the three-particle channel) this contribution grows rapidly with energy and markedly decreases the magnitude of the cross section at the resonance. The effect can be so large that the lower resonance in $T=\frac{1}{2}$ may be easily seen, experimentally, while the higher resonance in $T=\frac{3}{2}$ cannot be separated from the experimental errors, at least at present.

(6) Finally, it is of interest to examine the extreme cases when $\Gamma^J\rightarrow 0$ and Γ^J is very large. The first case, $\Gamma^J\rightarrow 0$, is of a trivial nature. Eq. (31) shows that all the F_{ij} are zero. This is not surprising; there is no inhomogeneous term to drive the unitarity relation, i.e., the integral equations. Said another way, all potentials between particles are zero. The case when Γ^J is very large is more interesting. Referring to Eq. (31), we find (for Γ^J very large)

$$\begin{aligned}&F_{22}(w)\rightarrow-(w-w_2)^{-1}[K_2(w,w_2)-K_2(w_2)]^{-1},\\ &F_{32}(w,\rho)\rightarrow 0,\\ &F_{33}(w,\rho,\rho')\rightarrow-\frac{1}{w-w_2}\frac{f(\rho)f^*(\rho')}{A\int d\rho''|f(\rho'')|^2[K_3(w,w_2;\rho'')-K_3(w_2,w_2;\rho'')]},\end{aligned}\tag{35}$$

where A is a factor involving the relations between the Γ^ζ, see Eq. (31). At first, it may seem strange that F_{23} is zero, since the coupling between the two- and three-particle channels is very large. However, consider a transition between a two- and three-particle state. Since the transition can be made, we should expect that F_{23} is nonzero. But the coupling is so strong that the three-particle state immediately makes a transition back to a two-particle state, and the transition will never be a permanent (asymptotic) one. Thus F_{23} is zero. In fact, when such strong coupling is present, there is a decoupling between two- and three-particle scattering. This may be seen by observing the analyticity in Eq. (35). In particular, F_{22} and F_{33} do not have the same cuts: F_{22} is cut from w_2, while F_{33} is cut from w_3. This particular difference in analyticity between two- and three-particle scattering makes a permanent transition between them impossible. Considering the

analyticity of Eq. (35) further, it would appear that both F_{22} and F_{33} have developed a pole at w_2 (if we had chosen the inelastic pole at $w_0<w_2$, then F_{22} and F_{33} would have poles at w_0), since the cancellation arising from the form of Eq. (32) is no longer present. However, the form given in Eq. (35) is invalid when $w=w_2$. To see this we note that we have, by definition,

$$\lim_{w\to w_2}(w-w_2)F_{32}{}^J(w,\rho)=\Gamma^J f(\rho), \tag{36}$$

but from Eq. (31)

$$\lim_{w\to w_2}(w-w_2)F_{32}{}^J(w,\rho) =\Gamma^J f(\rho)/[1-\bar{K}_2(w_2)\bar{G}_3(w_2)]. \tag{37}$$

Thus, in order for Eqs. (36) and (37) to be compatible, we have the limit

$$\lim_{w\to w_2}\bar{K}_2(w_2)\bar{G}_3(w_2)=0, \tag{38}$$

independent of Γ^J. Thus, Eq. (35) is replaced by $(w\to w_2)$

$$\begin{aligned} F_{22}{}^J(w)&\to\sum_{\xi''}|\Gamma^{J\xi''}|^2\int d\rho''\,|f(\rho'')|^2\int_{w_3}^{\infty}dw'\,\frac{\rho_3{}^I(w',\rho'')}{(w'-w_2)^3},\\ F_{32}{}^{J\xi}(w,\rho)&\to\Gamma^{J\xi}f(\rho)/(w-w_2),\\ F_{33}{}^{J\xi\xi'}(w,\rho,\rho')&\to\Gamma^{J\xi}\Gamma^{J\xi'}f(\rho)f^*(\rho')\int_{w_2}^{\infty}dw'\,\frac{\rho_2{}^L(w')}{(w'-w_2)^3}, \end{aligned} \tag{35'}$$

which is valid independent of Γ^J. Thus, the imposed analyticity in Eq. (23) is in fact maintained.

At this point it is necessary and important to extend the results of paragraph (6) outside the direct applicability of our model. In particular, let us consider the two cases in (6) when there is an elastic pole as well as an inelastic pole. We will take this elastic pole at $w=w_e<w_2$ with residue α^J. The general structure of the denominator common to all the amplitudes is

$$\begin{aligned}\Delta(w^2)=1&-\alpha[K_2(w,w_2)-K_2(w_e)]\\ &-[G_3(w,w_2)-G_3(w_2)][K_2(w,w_2)-K_2(w_2)]\\ &+\alpha\textstyle\sum_\xi|\Gamma^\xi|^2[\text{mixed terms in } G_3 \text{ and } K_2].\end{aligned} \tag{39}$$

Clearly, when $\alpha\to 0$, this is identical with the model given here. However, let us consider the extreme cases $\Gamma^J\to 0$ or Γ^J very large when $\alpha\neq 0$.

In contrast to paragraph (6), when $\Gamma\to 0$, F_{22} remains finite (since the numerator contains a term proportional to α as well as Γ^J) with a denominator of the form

$$\Delta(w^2)=1-\alpha[K_2(w,w_e)-K_2(w_e)], \tag{40}$$

and F_{23} and F_{33} go to zero. This is exactly the form that is obtained when one computes F_{22}, *neglecting* inelastic contributions, i.e., the unitarity relation is of the form

$$\mathrm{Im}F_{22}=\pi\rho_2{}^L|F_{22}|^2. \tag{41}$$

Referring to Fig. 4 and Eq. (33), this solution corresponds to setting $[\bar{G}(w,w_2)]^{-1}=1/\alpha$. Thus, it is not surprising that previous attempts to obtain resonances by nelgecting inelastic contributions have not been very successful,[13] at least when reasonable values of the left-hand discontinuities are used, i.e., values of α.

When we take the opposite case, Γ very large, the results are similar to those given in paragraph (6). However, we can interpret the result in a different way; this is again equivalent to neglecting the inelastic contributions to F_{22} since the unitarity condition is of the form of Eq. (41). This corresponds to setting $[\bar{G}_3]^{-1}=0$ in Eq. (33) and Fig. 4.

Finally, if Γ^J is finite and $\alpha\neq 0$ we can determine the behavior of the resonance as a function of α from Eq. (39). Specifically, if α is not too large, the position of the resonance will be at most shifted. If one is given the sign of α and can consider the mixed terms in Eq. (39) as negligible, then one can even determine whether the shift is to higher or lower energies.

C. Specific Solutions

It is now possible for us to describe the results of our calculations for specific choices of the $N-\rho$ system and the resulting π-N system. In particular, we wish to consider $I_J=0$ and 1, and more specifically the ρ-N states $S_{\frac{1}{2}}$ and $P_{\frac{3}{2}}$. As seen in Table I, these are connected to the π-N states $D_{\frac{3}{2}}$ and $F_{\frac{5}{2}}$, and we consider both values of the isotopic spin.

In order to obtain numerical solutions for the amplitudes we must calculate $K_2{}^L(w,w_2)$ and $G_3{}^I(w,w_2)$ for the combinations $(L,I)_J=(2,0)_{\frac{3}{2}}$ and $(3,1)_{\frac{5}{2}}$ as they are defined in Eqs. (26) and (16). Such integrals are difficult to perform by machine calculation, since they involve principal-value integrals and imaginary parts. This difficulty is particularily emphasized in the case of $G_3(w,w_2)$ which involves an additional integration over ρ. The complexity due to the ρ integration in G_3 can be eliminated by taking the $\pi-\pi$ system in a sharp resonance state and using Eq. (34). On the other hand, the difficulties associated with the principal-value integrals can be diminished by approximating the phase-space factors and performing the integration analytically. As shown in the Appendix, $\rho_2{}^L$ and $\rho_3{}^I$

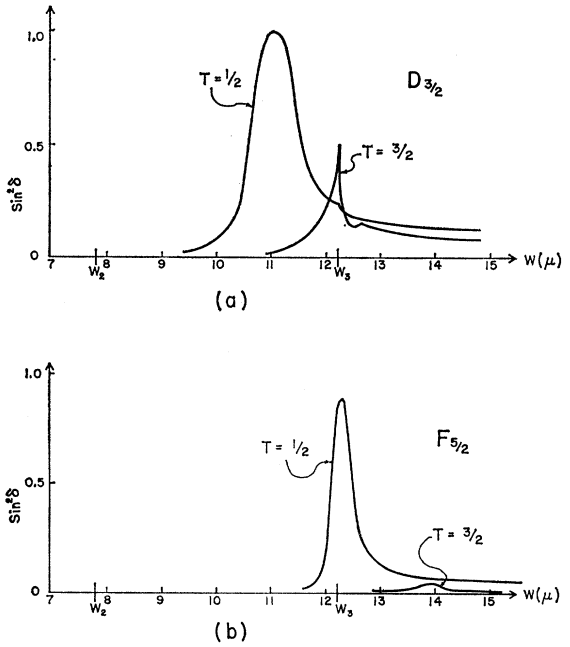

FIG. 5. Plot of $\sin^2\delta$ for $D_{\frac{3}{2}}$ and $F_{\frac{5}{2}}$ in elastic π-N scattering.

can be well approximated as

$$\begin{aligned}
\rho_2^{(2)}(w) &\simeq [2m/4(2\pi)^3](1/4w^3) \\
&\quad \times\{(w-m)^2-\mu^2]^2/(w+m)\} \\
&\quad \times[(w-m)^2-\mu^2]^{\frac{1}{2}}, \\
\rho_2^{(3)}(w) &\simeq [2m/4(2\pi)^3](1/4w^3) \\
&\quad \times\{[(w-m)^2-\mu^2]^3/(w+m)^3\} \\
&\quad \times[(w-m)^2-\mu^2]^{\frac{1}{2}}, \\
\rho_3^{(0)}(w,\rho_R) &\simeq [2m/32(2\pi)^6]^{\frac{1}{4}}[1+(m+\rho_R/w)] \\
&\quad \times[w^2-(m+\rho_R)^2]^{\frac{1}{2}}, \\
\rho_3^{(1)}(w,\rho_R) &\simeq [2m/32(2\pi)^6]^{\frac{1}{4}}[1-(m+\rho_R/w)] \\
&\quad \times[w^2-(m+\rho_R)^2]^{\frac{1}{2}}.
\end{aligned} \tag{42}$$

With this approximation for the phase-space factors the appropriate functions, K_2 and G_3, can be obtained explicitly, see Appendix. For both of the combinations of interest, viz., $(2,0)_{\frac{3}{2}}$ and $(3,1)_{\frac{5}{2}}$, the resulting curves are similar to those shown in Fig. 4. In Fig. 5 we show $\sin^2\delta$ for the $\pi-N$ states $D_{\frac{3}{2}}{}^T$ and $F_{\frac{5}{2}}{}^T$ with both values of the isotopic spin. For both $D_{\frac{3}{2}}$ and $F_{\frac{5}{2}}$ we have chosen the appropriate value of Γ^J to fit the experimental data for the $T=\frac{1}{2}$ states. As pointed out in Sec. III B the behavior of the $T=\frac{3}{2}$ states is automatically determined by the isotopic spin dependence of $f^T(\rho)$.

In the $D_{\frac{3}{2}}$ channel we have chosen an appropriate value of Γ so that the $T=\frac{1}{2}$ has a resonance at 600 MeV,[21,22] and since the isotopic spin dependence is determined we find a resonance in $T=\frac{3}{2}$ is also present. This $T=\frac{3}{2}$ resonance corresponds to a zero in the real part of the denominator of Eq. (33) at $w=12.6\mu$ (980 MeV), but because of the remarks in Sec. III B, paragraph (5), and the fact that $\rho_3^{(0)}(w,\rho_R)$ increases very rapidly above $w=m+\rho_R$, the maximum actually occurs at $w=m+\rho_R=12.2\mu$ (880 MeV). We would like to interpret this maximum (cusp) as the "knee" in the π^+p cross-section at $\simeq$850 MeV.[21,22] This rapid development of the inelastic channel (for $I=0$) is responsible for the cusp effect as well as the reduced cross-section of the $D_{\frac{3}{2}}^{(\frac{3}{2})}$ amplitude. Actually, the sharpness of the cusp is a spurious effect, and if we were to perform the ρ integration rather than using Eq. (34), the resonance curve would become a smooth function.

The resonance in the $F_{\frac{5}{2}}^{(\frac{1}{2})}$ channel is placed at $w=12.3\mu$ (900 MeV),[21,22] which is above the inelastic threshold (880 MeV). In contrast to the remarks pertinent to the $D_{\frac{3}{2}}$ channel, there is little reduction of the cross-section of the $F_{\frac{5}{2}}^{(\frac{1}{2})}$ amplitude. This follows simply from the fact that $\rho_3^{(1)}(w,\rho_R)$ does not increase as rapidly as $\rho_3^{(0)}(w,\rho_R)$ in the energy region, $w>m+\rho_R$. On the other hand, the accompanying resonance in the $F_{\frac{5}{2}}^{(\frac{3}{2})}$ channel occurs at $w=14.0\mu$ (1350 MeV), and is severely reduced since $\rho_3^{(1)}(w,\rho_R)$ is no longer negligible. It is thus likely that this resonance is responsible for the "resonance" near 1.4 BeV in the π^+p cross-section.[21,22]

We have pointed out that the value of Γ^J has been chosen so as to best represent the $T=\frac{1}{2}$ experimental data. However, an independent estimate of its magnitude can be obtained from Eqs. (17) and (21). From Eq. (20) we see that $x\to\infty$ as $P\to 0$ or $Q\to 0$, and in the limit $Q\to 0$, I^J is dominated by the $Q_n(x)$ with the lowest index in Eq. (19), i.e., $n=l-1$. We may thus obtain a value of Γ^J by comparing Eq. (21) with Eq. (17) when $Q\to 0$ and retain only those terms proportional to $Q_{l-1}(x)$. Since we have taken $\rho=\rho_R$, $Q\to 0$ corresponds to $w\to m+\rho_R$, and comparing Eq. (21) with Eq. (17), using Eq. (19), we obtain

$$\begin{aligned}
\Gamma_{\text{P.T.}}{}^{J1} &= (\rho_R-\mu)\lim_{\substack{w\to m+\rho_R \\ \rho\to\rho_R}}\{[(E+m)/P]^L[(Q_0+m)/Q]^I \\
&\quad \times 1/Q[P(E+m)]l/(2l+1)Q_l(x)\}, \\
\Gamma_{\text{P.T.}}{}^{J3} &= -\sqrt{2}\Gamma^{J1}, \\
\Gamma_{\text{P.T.}}{}^{J5} &= -[(l+2)/l]\Gamma^{J1}.
\end{aligned} \tag{43}$$

The values obtained from Eq. (43) are larger than those actually employed in Fig. 5:

$$\begin{aligned}
D_{\frac{3}{2}}&: \Gamma^{\frac{3}{2}1} \simeq \tfrac{2}{3}\Gamma_{\text{P.T.}}{}^{\frac{3}{2}1}, \\
F_{\frac{5}{2}}&: \Gamma^{\frac{5}{2}1} \simeq \tfrac{1}{5}\Gamma_{\text{P.T.}}{}^{\frac{5}{2}1}.
\end{aligned} \tag{44}$$

If the perturbation-theory values of Γ had been used, the resonances discussed in the preceding paragraphs would still be present, but at much lower energies. However, the disparity between the values of Γ is due in part to our method of comparing Eqs. (17) and (21).

[21] P. Falk-Vairant and G. Valladas, *Proceedings of the 1960 Annular International Conference on High-Energy Physics at Rochester* (Interscience Publishers, Inc., New York, 1960), page 38.

[22] C. D. Wood, T. J. Devlin, J. A. Helland, M. J. Longo, B. J. Moyer, and V. Perez-Mendez, Phys. Rev. Letters **6**, 481 (1961); other references are given in this paper.

In particular, as $w \to m+\mu$, we have seen that $F_{32}{}^J \to 1/P^{2L+2}$ which, for $L=2$, 3, is much faster than our pole approximation. It is likely that sizable errors have been introduced if the region near the elastic threshold is important in the w integration of $\bar{K}_2(w,w_2)$. This is particularly relevant when we realize that the amount of error introduced by the pole approximation increases as L increases. Our calculations tend to overestimate the value of $\bar{K}_2(w,w_2)$. A reduction of $\bar{K}_2(w,w_2)$ to compensate for this error would yield resonances at higher energies, and a fit of the data would be possible with less disparity between Γ and $\Gamma_{\text{P.T.}}$.

IV. CONCLUSIONS

In this article we have attempted to explicate the role played by production amplitudes in the determination of elastic amplitudes when they are coupled by unitarity. We have also endeavored to demonstrate the importance of this elastic-inelastic coupling by means of an explicit calculation. The most pertinent observation that can be obtained from our analysis concerns the importance of the left-hand discontinuities relative to the restrictions imposed by unitarity. In particular, it is likely in many processes that the elastic "forces" contribute very little to the structure of the elastic amplitude near the thresholds of inelastic channels. It is rather the particular form of the coupling between the amplitudes, i.e., the unitarity relations, which is responsible for their structure.

It does not follow that this observation is generally applicable, and an important exception may be $\pi-\pi$ scattering where the elastic "forces" are very dependent on the crossing relations, i.e., when an additional constraint, which can be very restrictive, is imposed on the system, the unitarity relation may not be sufficient to determine the general properties of the amplitudes. On the other hand, we believe it very plausible that the strange-particle resonances observed recently[23] are the result of the coupling between the various strange-particle channels and not specific left-hand singularities. It is true that several channels must be considered in the scattering of strange particles and the analysis is more complicated, but this implies that the constraints imposed by unitarity are more severe than ever. In this connection, it is important to realize that any inelastic channel can restrict the form of the elastic amplitude, i.e., two-particle as well as three-particle channels. As in the work of Dalitz,[5] it seems likely that the resonance in the $\pi-\Lambda$ systems can be understood in terms of coupling to the $\bar{K}-N$ and $\pi-\Sigma$ channels.

A comparison between the model presented here and the works of others[3–5,7,13–15] is most conveniently made by referring to the remarks in the previous paragraphs. In particular, we take as fundamental the unitarity relations, and insist that these relations be rigorously satisfied (at least in the truncated form), while other authors have attempted to emphasize different aspects of particular problems at the expense of the unitarity relations. An important property, which follows from the unitarity coupling and is not shared by procedures that neglect this coupling, is the marked decrease in the cross section above the inelastic threshold. Such behavior can be explicitly included in any given calculation, but an *ad hoc* procedure of this type will surely violate the unitarity relations at some other stage of the calculation. One must satisfy the unitarity relations at the onset of the analysis and maintain them throughout.

This rapid increase in the inelastic absorption with the resulting decrease in the elastic cross section is partially responsible for our emphasis on coupling the three-particle system as $(\pi\pi)N$ rather than $\pi(\pi N)$.[14] It is true that the formation of the (3,3) isobar takes place in the production reaction. However, it is not obvious that it dominates the production reaction and elastic scattering above 400 MeV (pion laboratory kinetic energy). In fact, if we consider the (3,3) isobar as a sharp resonance with a "mass" of 9μ and perform a calculation similar to that in Sec. III, then the inelastic threshold occurs at about 10μ (390 MeV) and any resonant behavior in the elastic channel much above that energy will be reduced to a very small value (as the $T=\frac{3}{2}$, $F_{\frac{5}{2}}$ resonance in Fig. 5). Thus, it seems unlikely that the (3,3) isobar formation is very significant in the development of the higher $\pi-N$ resonances.

The preceding remarks suggest the following statement: In general, when an elastic channel is coupled to a set of inelastic channels in such a way that resonances result, the position of an observable resonance will be essentially at or below the inelastic threshold. This statement is in contrast to the conclusion of Ball and Frazer,[3] and a few additional remarks are necessary. The basic observation made by them is that a rapidly rising, inelastic cross section will lead to a resonance in the elastic channel. Because this resonance is a result of a particular analyticity, the resonance occurs very near the region of the rapid increase. By an appropriate choice of the inelastic absorption, they then fit the elastic data. Unfortunately, the magnitude of the inelastic absorption is chosen rather arbitrarily. The pertinent remark in a comparison of their model with the model presented here is that the rapidly rising, inelastic cross section in their model represents the *real* production of an N and ρ. For this reason, the location of the elastic resonance cannot be very different from the inelastic threshold (thus, they must choose the $\pi-\pi$ system as resonating between 4.5 and 5μ, so that the inelastic threshold, 11.3μ (670 MeV) $<w^T$ $<11.8\mu$ (780 MeV), is not very much larger than the 600-MeV resonance). On the other hand, in the model presented here, the elastic amplitude can resonate far below the inelastic threshold by means of the *virtual*

[23] See, e.g., M. H. Alston, L. W. Alvarez, P. Eberhard, M. L. Good, W. Graziano, H. K. Ticho, and S. J. Wojcicki, Phys. Rev. Letters **5**, 520 (1960); O. Dahl, N. Horwitz, D. H. Miller, J. J. Murray, and D. G. White, *ibid.* **6**, 142 (1961).

production of an N and ρ. It is this virtual production which is allowed by the unitarity relations, and is not present in the work of Ball and Frazer. Of course, how the inelastic amplitude develops the necessary energy dependence in their model cannot be discussed, while here it is the unitarity coupling between the channels which is responsible.

In Sec. I we mentioned an alternative mechanism to that presented here, i.e., a bound state in one channel decaying into another channel.[5,7] While such a mechanism may describe certain experimental effects, it differs from the model presented here in an essential way. In the analysis, e.g., presented by Sakurai,[7] the tacit assumption is made that it is possible to separate one channel from another and discuss the interaction between them in terms of decaying systems. In contrast to this point of view, we consider as basic a strong coupling between the channels; in fact, this coupling is so strong that any effective separation between the channels is impossible. Thus, although it may be possible to phrase some of our results in terms of a bound-state mechanism, an essential difference in outlook is present.

A final comparison can be made with the model of peripheral collisions.[24] Because of the specific coupling chosen between the elastic and inelastic channels (Fig. 2), it would appear that a definite connection to peripheral-collision models is present. However, the rigorous application of the unitarity relations implies that any number of pions, compatible with symmetry principles, can be exchanged in M_{22}, M_{23}, and M_{33}. There is thus little comparison between the models.

Finally, it is of interest to discuss the relevance of the particular choice of singularities and coupling made here to the experimental results. We have already discussed the difficulty associated with the coupling $\pi(\pi N)$. Similar remarks can be made about the channels[25] $N+\eta$ and[26] $N+\zeta$, although they might have some effect on the 600 MeV, $T=\frac{1}{2}$ resonance. These remarks do not apply to the channel $N+\omega$. However, since ω has $T=0$, the "knee" in the $T=\frac{3}{2}$ could not develop, i.e., the isotopic spin dependence of $f^T(\rho)$ does not allow a contribution to the $T=\frac{3}{2}$ state. Thus, of the inelastic channels which could be the relevant ones to actually reproduce the data, the channel $N+\rho$ is certainly most favored. It is important to emphasize that the model developed here cannot determine which inelastic channel is most strongly coupled to the elastic channel. This is an assumption, *a priori*, and must be checked against the data.

The above remarks and the results of Sec. III C provide rather strong evidence that the $N+\rho$ channel is most strongly coupled to the $N+\pi$ channel. However, Table I implies a certain arrangement of partial waves. The calculations in Sec. III C consider $I_J=0$, 1 for the largest J-value allowed. However, we should also expect that the $S_{\frac{1}{2}}$, $\pi-N$ channel is driven by $I_J=0$ as well as $D_{\frac{3}{2}}$ [we would not necessarily expect a resonance in these additional partial waves because of the behavior of $\rho_2{}^L(w)$]. Experimentally,[22] it is necessary to mix $S_{\frac{1}{2}}$ and $D_{\frac{3}{2}}$ waves to fit the data which is quite satisfactory.

On the other hand, $I_J=1$ will drive $P_{\frac{1}{2}}$ and $P_{\frac{3}{2}}$ as well as $F_{\frac{3}{2}}$, but no D waves. Unfortunately, the experimental evidence[22] shows that a strong mixing of D waves with the predominant $F_{\frac{3}{2}}$ wave is necessary (with perhaps some P wave). Only if $I_J=2$ can any D waves be introduced into the 900-MeV resonance. However, this possibility is unlikely for the following reason: We have seen that the position of the resonance for $I_J=1$ is higher than that for $I_J=0$. It is likely then that a resonance for $I_J=2$ would be at an even higher energy, with a value of Γ^J not very different from $\Gamma_{\text{P.T.}}{}^J$, and thus would produce no strong D-wave scattering at 900 MeV. Further, it is possible that one would not see such a resonance because of the inelastic absorption. Incidentally, the $N+\rho$ channel can have no effect on the resonance in the $T=\frac{3}{2}$ channel near 1.4 BeV. Again, the reason is the large absorption of the inelastic channel.

The most obvious extension of the particular calculation presented in Sec. III would be the inclusion of another channel. An example, and in the nature of a conjecture, would be to include a coupling of the $N+3\pi$ system, other than that mentioned previously, to the πN channel, viz., $(N\pi)(\pi\pi)$, where the $(N\pi)$ system is the (3,3) isobar and the $(\pi\pi)$ system is the ρ meson. As with $(\pi\pi)N$, the isotopic-spin dependence of $f^T(\rho)$ is approximately 1 for $T=\frac{3}{2}$ and 2 for $T=\frac{1}{2}$. If we consider the lowest states, i.e., $I_J=0$, then we find that $S_{\frac{1}{2}}$, $D_{\frac{3}{2}}$, and $D_{\frac{5}{2}}$ are the corresponding πN channels. Again the $T=\frac{1}{2}$ channel will have its resonance at a lower energy than that in the $T=\frac{3}{2}$ channel. In this case, the reduction of the elastic cross section above 900 MeV, because of a large inelastic absorption, does not apply. To see this we consider both systems as sharp resonances, and find that the inelastic threshold occurs at $w=14.4\mu$ (1460 MeV). This situation is very attractive since we could consider a resonance at 900 MeV in the $T=\frac{1}{2}$ channel (providing the necessary D-wave mixing) and an additional resonance in the $T=\frac{3}{2}$ channel. It is not inconceivable that this $T=\frac{3}{2}$ resonance would be the resonance near 1.4 BeV in π^+p scattering, in which case the angular distribution would be dominated by $D_{\frac{5}{2}}$ and $D_{\frac{3}{2}}$.

[24] S. D. Drell, Revs. Modern Phys. **33**, 458 (1961).
[25] A. Pevsner, R. Kraemer, M. Nussbaum, C. Richardson, P. Schlein, R. Strand, T. Toohig, M. Block, A. Engler, R. Gessaroli, and C. Meltzer, Phys. Rev. Letters **7**, 421 (1961).
[26] R. Barloutaud, J. Heughebaert, A. Leveque, J. Meyer, and R. Omnes (to be published).

ACKNOWLEDGMENTS

The authors have benefited by conversations with Professor R. Blankenbecler, Professor M. Froissart, Professor M. L. Goldberger, and Professor S. B. Treiman.

Part of this work was done during the authors' stay at the Brookhaven National Laboratory in the summer, 1961, and both authors wish to thank Professor M. Goldhaber and Professor G. C. Wick for the hospitality extended to them there. One of the authors (B. W. L.) wishes to thank Professor J. R. Oppenheimer for the hospitality extended to him at The Institute for Advanced Study.

APPENDIX

We wish to rewrite and approximate the phase-space factors in a somewhat more convenient form. The explicit forms are, suppressing the θ functions and the factors of (2π),

$$\rho_2{}^L(w)=[P^{2L+1}/w(E+m)^{2L-1}]$$
$$=\frac{1}{w}\frac{[(w-m)^2-\mu^2]^{L+\frac{1}{2}}[(w+m)^2-\mu^2]^{L+\frac{1}{2}}}{(2w)^{2L+1}}\times\frac{(2w)^{2L-1}}{[(w+m)^2-\mu^2]^{2L-1}}, \quad \text{(A1)}$$

and

$$\rho_3{}^I(w,\rho)=[Q^{2I+1}/w(Q_0+m)^{2I-1}]$$
$$=\frac{1}{w}\frac{[w^2-(m+\rho)^2]^{I+\frac{1}{2}}[w^2-(m-\rho)^2]^{I+\frac{1}{2}}}{(2w)^{2I+1}}\times\frac{(2w)^{2I-1}}{[(w+m)^2-\rho^2]^{2I-1}}. \quad \text{(A2)}$$

We consider $\rho_2{}^L(w)$ first and use the approximation

$$[(w+m)^2-\mu^2]\simeq(w+m)^2. \quad \text{(A3)}$$

Then from Eq. (A1)

$$\rho_2{}^L(w)\,(1/4w^3)\{[(w-m)^2-\mu^2]^L/(w+m)^{2L-3}\}\times[(w-m)^2-\mu^2]^{\frac{1}{2}}. \quad \text{(A4)}$$

In the case of $\rho_3{}^I(w,\rho)$, since we take $\rho=\rho_R=5.4\mu$, we use the approximation

$$[w^2-(m-\rho)^2]\simeq w^2. \quad \text{(A5)}$$

From Eq. (A2), we obtain

$$\rho_3{}^I(w,\rho)\simeq\frac{1}{2^{2I}(2w)^{2-2I}}\frac{[w^2-(m+\rho)^2]^I}{[(w+m)^2-\rho^2]^{2I-1}}\times[w^2-(m+\rho)^2]^{\frac{1}{2}}. \quad \text{(A6)}$$

For $I=0$, we use the approximation

$$[(w+m)^2-\rho^2]/w^2\simeq 1+(m+\rho)/w;$$

thus

$$\rho_3{}^{(0)}(w,\rho)=\tfrac{1}{4}[1+(m+\rho)/w][w^2-(m+\rho)^2]^{\frac{1}{2}}. \quad \text{(A7)}$$

For $I=1$, we have

$$\rho_3{}^{(1)}(w,\rho)=\tfrac{1}{4}[(w-m-\rho)/(w+m-\rho)][w^2-(m+\rho)^2]^{\frac{1}{2}},$$

which can be well approximated as

$$\rho_3{}^{(1)}(w)\simeq\tfrac{1}{4}[1-(m+\rho)/w][w^2-(m+\rho)^2]^{\frac{1}{2}}. \quad \text{(A8)}$$

Using the approximate forms of the phase-space factors, it is straight-forward calculation to determine the functions $K_2{}^L(w)$ and $G_3{}^I(w)$. Consider, for example, $\bar{K}_2{}^{(3)}(w)$; we have

$$\bar{K}_2{}^{(3)}(w)=\frac{(w-w_2)}{4}\int_{w_2}^{\infty}\frac{dw'}{w'-w}[(w'-m)^2-\mu^2]^{\frac{1}{2}}\times\left[\frac{(w'-m+\mu)^3(w'-w_2)}{w'^3(w'+m)^3}\right], \quad \text{(A9)}$$

which becomes, when written in partial fractions,

$$\bar{K}_2{}^{(3)}(w)=\frac{(w-w_2)}{4}\int_{w_2}^{\infty}\frac{dw'}{w'-w}[(w'-m)^2-\mu^2]^{\frac{1}{2}}\times\left[\frac{A}{w'+m}+\frac{B}{(w'+m)^2}+\frac{C}{(w'+m)^3}+\frac{\alpha}{w'}+\frac{\beta}{w'^2}+\frac{\gamma}{w'^3}\right]. \quad \text{(A10)}$$

Defining the function,

$$H(w,\tau)=Partie\ finie\int_{w_2}^{\infty}dw'\frac{[(w'-m)^2-\mu^2]^{\frac{1}{2}}}{(w'-w)(w'-\tau)},$$

we obtain

$$\bar{K}_2{}^{(3)}(w)$$
$$=\tfrac{1}{4}(w-w_2)[AH(w,-m)+B[\partial H(w,\tau)/\partial\tau]|_{\tau=-m}+(C/2)[\partial^2H(w,\tau)/\partial\tau^2]|_{\tau=-m}+\alpha H(w,0)+\beta[\partial H(w,\tau)/\partial\tau]|_{\tau=0}+(\gamma/2)[\partial^2H(w,\tau)/\partial\tau^2]|_{\tau=0}].$$

$H(w,\tau)$ can be explicitly evaluated analytically, and thus $\bar{K}_2{}^{(3)}(w)$. A similar procedure may be used to evaluate all the appropriate K's and G's.

Notes added in proof. (1) Professor W. R. Frazer and Dr. J. S. Ball have kindly pointed out to us that the solution for $F_{22}(w)$ in Eq. (33) has a "ghost pole" at some real value of w, since as $w\to-\infty$, $\bar{K}_2(w)$ goes to $-\infty$ logarithmically, while $[\bar{G}_3(w)]^{-1}$ is negative for $w<w_3$ and goes to zero in that limit. (2) The quantities $K_2(w,w_2)$ and $G_3(w,w_2)$ are actually divergent. In the final solution, Eq. (31), only the subtracted forms appear, so that the formal manipulation from Eq. (27) through Eq. (31) is justified. We could of course have made a subtraction in the matrix **D** and avoid handling divergent quantities.